Photochemical & Photobiological Sciences

PAPER

Cite this: *Photochem. Photobiol. Sci.*, 2018, **17**, 1247

A multifunctional selective "turn-on" fluorescent chemosensor for detection of Group IIIA ions Al^{3+}, Ga^{3+} and In^{3+}†

Hyo Jung Jang, Ji Hye Kang, Dongju Yun and Cheal Kim *

Received 23rd April 2018,
Accepted 17th July 2018

DOI: 10.1039/c8pp00171e

rsc.li/pps

A versatile chemosensor **1** (*E*)-2-(((8-hydroxy-2,3,6,7-tetrahydro-1*H*,5*H*-pyrido[3,2,1-*ij*]quinolin-9-yl)methylene)amino)-1*H*-benzo[*de*]isoquinoline-1,3(2*H*)-dione, based on naphthalimide and julolidine moieties, was developed for highly distinguishable and selective recognition of Group IIIA metal ions (Al^{3+}, Ga^{3+} and In^{3+}). Sensor **1** exhibited significant 'off–on' fluorescence responses at 488 nm in the presence of Al^{3+} and at 570 nm in the presence of Ga^{3+} and In^{3+}. The same emission of Ga^{3+} and In^{3+} could be distinguished through different color changes (from colorless to yellow for Ga^{3+} and no color change for In^{3+}). Binding constants of **1** for Ga^{3+} and In^{3+} are the highest reported to date for an organic chemosensor. A 2 : 1 binding mode between **1** with Al^{3+}, Ga^{3+} and In^{3+} is proposed based on electrospray ionization mass spectrometry, Job plot analysis, and theoretical calculations.

1. Introduction

Development of a selective chemosensor capable of detection of trivalent metal ions in Group IIIA such as Al^{3+}, Ga^{3+} and In^{3+} is of interest since various roles are played by these metal ions in a broad range of biological and environmental processes.[1,2] For instance, aluminum is extensively used in daily life, for example in water purification, manufacturing industry, and food packaging.[3,4] Owing to its extensive use, it can be easily accumulated into human body and is toxic to humans in excessive amounts.[5–7] The excessive accumulation of Al^{3+} in the brain can lead to neurodementia, including neurological damages such as Alzheimer's and Parkinson's diseases.[8–10] Thus, there is strong demand for a highly sensitive and selective chemosensor for Al^{3+}.[11–19]

Gallium, a silvery metal, is extensively applied in chemical synthesis, fuel storage and the semiconductor industry, for example in light-emitting diodes and lasers.[20,21] Moreover, its nitrate salt has been used as an antitumor pharmaceutical owing to the high affinity of gallium for tumors.[22] Though the physiological function of gallium in the human body is not known, there is no doubt that it is carcinogenic and toxic to animals and humans. Chronic exposure to gallium causes severe disease, such as gastrointestinal disease, coma, anemia, leucopenia and skin cancer, and sometimes death.[23] Therefore, it is essential to design and synthesize sensors for detecting Ga^{3+}.[23–27]

Indium, a lustrous and malleable metal, has been widely used in many industrial fields, for example in transparent electrically-conductive films and gas sensors.[28,29] However, In^{3+} has direct impacts on sites of absorption, storage, transportation and utilization in cells, causing interference with Fe^{3+} metabolism.[30,31] To date, several chemosensors for indium have been developed, but many of them still have trouble distinguishing In^{3+} from Al^{3+} and Ga^{3+} owing to their similar physical properties.[32] Thus, it still remains a huge challenge to develop novel chemosensors with high sensitivity and selectivity for In^{3+} detection.

In recent year, research in the chemosensor field has extensively focused on development of multifunctional sensors, because they are more effective and economical than sensors with single-ion responses.[33–45] Nevertheless, most multifunctional sensors for the trivalent metal ions Al^{3+}, Ga^{3+} and In^{3+} have difficulty in distinguishing between them because of their similar physical properties.[46–50]

Herein, we report a multifunctional fluorescent chemosensor **1** based on the combination of napthalimide and julolidine for the detection of Group IIIA metal ions (Al^{3+}, Ga^{3+} and In^{3+}). Sensor **1** showed discernible fluorescence enhancement toward Al^{3+}, Ga^{3+} and In^{3+} over various metal ions. Importantly, **1** can differentially detect Al^{3+}, Ga^{3+} and In^{3+} at two different wavelengths along with a difference in color change. Sensing mechanisms of Al^{3+}, Ga^{3+} and In^{3+} are proposed based on various spectroscopic methods and theoretical calculations.

Department of Fine Chemistry, Seoul National University of Science and Technology, Seoul 139-742, Korea. E-mail: chealkim@seoultech.ac.kr; Fax: +82-2-973-9140; Tel: +82-2-970-6693

†Electronic supplementary information (ESI) available. See DOI: 10.1039/c8pp00171e

2. Experiments

2.1. Instruments and materials

All chemicals were commercially available from Sigma-Aldrich. Fluorescence spectra were obtained with a PerkinElmer spectrophotometer. A PerkinElmer UV-vis spectrometer was used to obtain absorption spectra. ^{13}C and ^{1}H NMR spectra and ESI-MS data were collected with a Varian spectrometer and a Thermo Finnigan MAX quadrupole machine.

2.2. Synthesis of sensor 1 ((*E*)-2-(((8-hydroxy-2,3,6,7-tetrahydro-1*H*,5*H*-pyrido[3,2,1-*ij*]quinolin-9-yl)methylene)amino)-1*H*-benzo[*de*]isoquinoline-1,3(2*H*)-dione)

Compound **2** (2-amino-1*H*-benzo[*de*]isoquinoline-1,3(2*H*)-dione) was synthesized according to the literature method (Scheme 1).[51] Yield: 0.22 g (52.38%); ^{1}H NMR (DMSO-d_6): δ 8.42 (doublet, J = 8 Hz, 2H), 7.86 (triplet, J = 8 Hz, 2H), 8.49 (doublet, J = 8 Hz, 2H), 5.78 (singlet, 2H). Compound **1** was obtained from the reaction of **2** (0.11 g, 0.5 mmol), 8-hydroxyjulolidine-9-carboxaldehyde (0.7 mmol, 0.16 g) and five drops of H_3PO_4 in methanol. The reaction mixture was stirred for half a day at 20 °C. A pale orange precipitate was filtered, washed four times with ether, and dried to give the pure product. Yield: 0.07 g (34.1%); ^{1}H NMR (DMSO-d_6): δ 11.55 (s, 1H), 8.52 (m, 5H), 7.89 (t, J = 4 Hz, 2H), 6.82 (s, 1H), 3.24 (s, 4H), 2.62 (t, J = 4 Hz, 4H), 1.86 (q, 4H); ^{13}C NMR (DMSO-d_6): δ 172.75, 151.18, 156.84, 147.56, 135.02, 131.81, 130.58, 106.12, 105.10, 49.80, 49.34, 26.98, 21.72, 20.83, 20.47. ESI-MS: m/z $[\mathbf{1} + H^+ + 3{\cdot}H_2O + MeCN]^+$ calcd 507.22, found, 507.23.

2.3. Fluorescence titrations

A stock solution of **1** (0.005 mmol, 2.05 mg) was prepared in dimethyl sulfoxide (DMSO) (1 mL). 12 μL of the sensor solution (5 mM) was diluted with 2.98 mL methanol to afford a 20 μM solution. $Al(NO_3)_3$ (0.02 mmol) was dissolved in methanol (1 mL). 6–66 μL of the Al^{3+} solution (20 mM) was transferred into probe **1** solution (20 μM, 3 mL). After stirring for 5 s, fluorescence spectra were measured. Similar experimental methods were also applied for Ga^{3+} and In^{3+}.

2.4. UV-vis titrations

A stock solution of **1** (0.005 mmol, 2.05 mg) was prepared in DMSO (1 mL). 12 μL (5 mM) of the sensor solution was diluted with 2.98 mL methanol to give a 20 μM solution. $Al(NO_3)_3$ (0.02 mmol) was dissolved in methanol (1 mL). 3–30 μL (20 mM) of the Al^{3+} solution were transferred into probe **1** solution (20 μM, 3 mL). After stirring for 5 s, UV-vis spectra were measured. Similar experimental methods were also applied for Ga^{3+} and In^{3+}.

2.5. Job plot

A stock solution of **1** (0.005 mmol, 2.05 mg) was prepared in DMSO (1 mL). 120 μL of the probe **1** solution (5 mM) was diluted with 28.8 mL methanol to afford a 20 μM solution. 2.7–0.3 mL, at regular intervals, of the diluted probe **1** was added to quartz cells. 30 μL (20 mM) of $Al(NO_3)_3$ solution was diluted with 29.97 mL methanol. 0.3–2.7 mL, at regular intervals, of the diluted Al^{3+} solution was taken and added to each probe **1** sample. Each cell was filled with methanol to afford a total volume of 3 mL. After stirring for 5 s, fluorescence spectra were measured. Similar experimental methods were also applied for Ga^{3+} and In^{3+}.

2.6. Competition experiments

A stock solution of **1** (0.005 mmol, 2.05 mg) was prepared in DMSO (1 mL). 12 μL of the probe solution (5 mM) was diluted with 2.98 mL methanol to afford a 20 μM solution. 0.02 mmol of MNO_3 (M = Ag, Na and K) or $Fe(ClO_4)_2$ or $M(NO_3)_2$ (M = Pb, Ca, Ni, Hg, Mg, Cd, Zn, Co, Cu and Mn) or $M(NO_3)_3$ (M = In, Ga, Cr, Fe and Al) was dissolved in methanol (1 mL). 66 μL of each metal-ion solution (20 mM) was added to 3 mL of probe **1** (20 μM). Then, 66 μL of the Al^{3+} solution (20 mM) was taken and added to the mixture of each ion and probe **1**. After stirring for 5 s, fluorescence spectra were measured. Similar experimental methods were also applied for Ga^{3+} and In^{3+}.

2.7 Theoretical calculations

Density functional theory (DFT) and time-dependent DFT (TD-DFT) were used for theoretical calculations using the Gaussian 09 program.[52] On the basis of the hybrid exchange–correlation functional B3LYP,[53,54] the main elements were considered with the 6-31G (d, p) set,[55,56] and the aluminum, gallium and indium elements were considered for the LANL2DZ effective core potential (ECP).[57–59] The solvent effects of MeOH were applied to all calculations by using the CPCM (Cossi and Barone's conductor-like polarizable continuum model).[60,61] In order to explore the transition energies of the minimized structures of **1**, Al^{3+}-2·**1**, Ga^{3+}-2·**1** and In^{3+}-2·**1** complexes, the lowest 12 singlet–singlet transitions were examined by TD-DFT calculations in the ground state geometry (S_0). The contribution of molecular orbitals (MOs) was analyzed by GaussSum 2.2.[62]

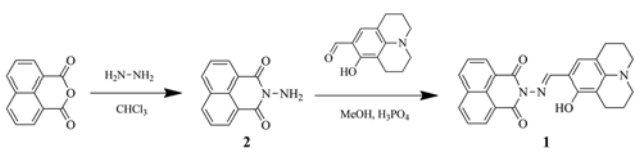

Scheme 1 Synthetic procedure of **1**.

3. Results and discussion

Compound **2** was prepared by the substitution reaction of 1,8-naphthalenedicarboxylic anhydride and hydrazine hydrate according to the literature,[51] and sensor **1** was also obtained by the substitution reaction of **2** and 8-hydroxyjulolidine-9-carboxaldehyde with 34.1% yield in MeOH (Scheme 1). Sensor **1** was characterized by electrospray ionization mass spectrometry (ESI-MS), ^{1}H and ^{13}C NMR (Fig. S1a and 1b†) analyses.

3.1. Fluorescence studies of 1 with Al^{3+}

We studied the fluorescence selectivity of **1** to various metal ions (Zn^{2+}, Cu^{2+}, Cd^{2+}, In^{3+}, Fe^{2+}, K^{+}, Na^{+}, Mg^{2+}, Pb^{2+}, Cr^{3+}, Co^{2+}, Ni^{2+}, Fe^{3+}, Ca^{2+}, Mn^{2+}, Al^{3+}, Ga^{3+}, Ag^{+} and Hg^{2+}) in MeOH with excitation at 368 nm (Fig. 1). Upon the addition of various metal ions to sensor **1** solution, Al^{3+} emitted bright blue–green fluorescence at 488 nm. Ga^{3+} and In^{3+} showed some fluorescence enhancements along with yellow–orange fluorescence. In^{3+} displayed the most red-shifted fluorescence, probably due to its heavy mass. In contrast, other metal ions displayed no significant spectral changes. The fluorescence response of **1** to Al^{3+} took about 10 min (Fig. S2†). These results demonstrated that probe **1** could be utilized as a "turn-on" chemosensor for Al^{3+} over the metal ions tested.

To examine the chemosensing properties of **1**, fluorescence titration of **1** with Al^{3+} was carried out (Fig. 2). With increasing amounts of Al^{3+}, the fluorescence of **1** gradually increased at 488 nm and reached a maximum at 22 equiv. of Al^{3+}. The photophysical properties of **1** were also studied by variations in the UV-vis spectrum of **1** upon treatment with Al^{3+} (Fig. 3). Upon gradual addition of Al^{3+} (0–9 equiv.) to sensor **1** solution, the absorbance peak of **1** at 367 nm steadily shifted to 412 nm, creating a new absorption band, which was accompanied by two clear isosbestic points at 268 nm and 384 nm. This observation indicated the formation of a single species. The absorbance maximum attained saturation with 8 equiv. of Al^{3+}.

The complexation mode of **1** with Al^{3+} was investigated using Job plot analysis,[63] which showed a 2 : 1 binding mode (Fig. S3†). The 2 : 1 complexation between **1** and Al^{3+} was further supported by ESI-MS. As shown in Fig. S4,† a peak at m/z = 847.40 was indicative of $[2\cdot\mathbf{1} + Al^{3+}\text{-}2H^{+}]^{+}$ (calcd 847.28). Using the results of fluorescence titration, the binding constant of **1** with Al^{3+} was calculated with Li's equation (see ESI†) and determined to be 3.0×10^{7} M^{-2} (Fig. S5†).[64] The detection limit of **1** for Al^{3+} was found to be 14.79 μM using 3σ/slope analysis (Fig. S6†).[65] Based on ESI-MS, Job plot analysis and UV-vis titration, we propose a possible structure for Al^{3+}-2·**1** (Scheme 2).

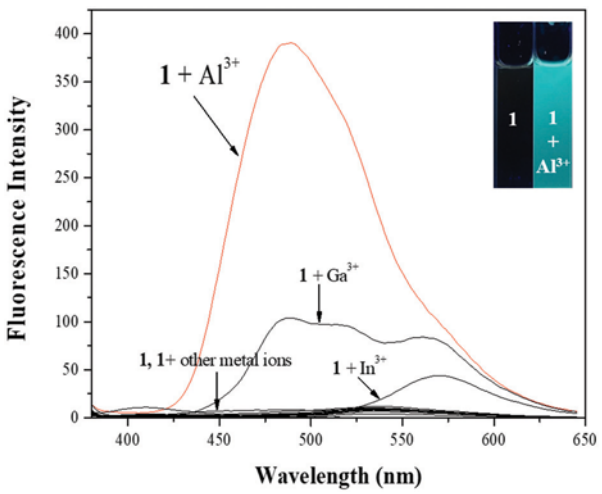

Fig. 1 Fluorescence spectral changes of **1** (20 μM) in the presence of various metal ions (22 equiv. Zn^{2+}, Cd^{2+}, In^{3+}, Cu^{2+}, Fe^{2+}, K^{+}, Na^{+}, Mg^{2+}, Pb^{2+}, Cr^{3+}, Co^{2+}, Ni^{2+}, Fe^{3+}, Ca^{2+}, Mn^{2+}, Al^{3+}, Ga^{3+}, Ag^{+} and Hg^{2+}) with an excitation of 368 nm.

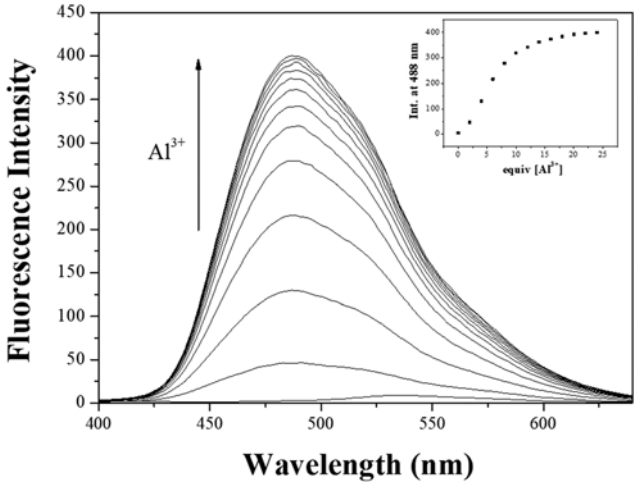

Fig. 2 Fluorescence spectral changes of **1** (20 μM) in the presence of various concentrations of Al^{3+} ions, with an excitation of 368 nm. Inset: Fluorescence intensity (488 nm) *vs.* the number of 22 equiv. of Al^{3+} added.

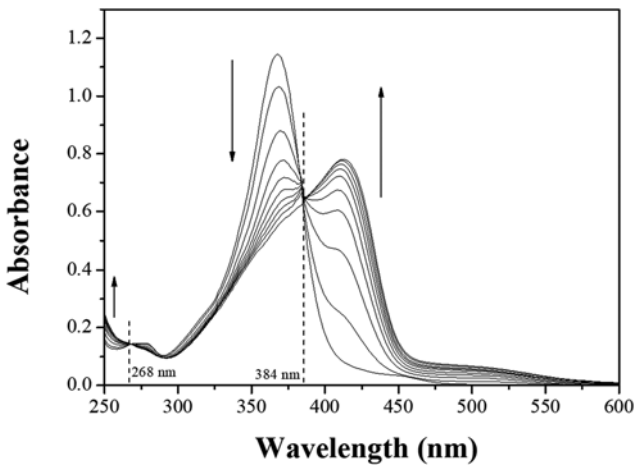

Fig. 3 UV-vis spectral changes of **1** (20 μM) in the presence of different concentrations of Al^{3+} ions.

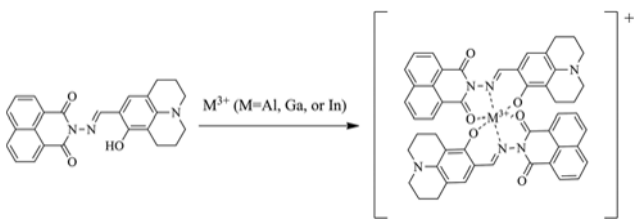

Scheme 2 Proposed binding mode of M^{3+}-2·**1** (M = Al, Ga or In) complexes.

To investigate the selectivity of **1** for Al^{3+}, competition experiments were conducted (Fig. S7†). When sensor **1** solution was treated with Al^{3+} in the presence of various metal ions, no or minor interference was observed for most competing metal ions. However, In^{3+}, Cu^{2+}, Cr^{3+} and Hg^{2+} inhibited 25–45% of the emission intensity of Al^{3+}-2·**1**, but the fluorescence intensity was still visible in their presence. Ga^{3+}, Fe^{2+} and Fe^{3+} quenched 74%, 77% and 64% of the fluorescence intensity.

3.2. Fluorescence studies of 1 with Ga^{3+} and In^{3+}

We changed the excitation wavelength from 368 nm to 481 nm, to further examine the fluorescence variation of **1** in response to various metal ions (Zn^{2+}, Hg^{2+}, Cd^{2+}, Cu^{2+}, Fe^{2+}, K^{+}, Na^{+}, Mg^{2+}, Pb^{2+}, Cr^{3+}, Co^{2+}, Ni^{2+}, Fe^{3+}, Ca^{2+}, Mn^{2+}, Al^{3+}, Ga^{3+}, Ag^{+} and In^{3+}) (Fig. 4). Among the various ions tested, **1** showed remarkable selectivity only for Ga^{3+} and In^{3+} by strong fluorescence enhancement at 570 nm. By contrast, no fluorescence response to other metal ions was observed. The fluorescence responses of **1** to Ga^{3+} and In^{3+} occurred within a few seconds. Fortunately, it is possible to distinguish Ga^{3+} from In^{3+} through color change. When Ga^{3+} and In^{3+} ions were added to sensor **1**, Ga^{3+} exhibited a unique color change from colorless to yellow (Fig. S8†). Most sensors for Al^{3+}, Ga^{3+} and In^{3+} generally show both a nearly identical fluorescence change at the same position and the same color change. Thus, this is the first report that a single chemosensor can simultaneously detect and differentiate between Al^{3+}, Ga^{3+} and In^{3+} in Group IIIA.

First of all, to study the fluorescence sensing behavior of **1** to Ga^{3+}, fluorescence and UV-vis titrations were carried out. The fluorescence emission at 570 nm constantly increased up to 9 equiv. of Ga^{3+} (Fig. 5). Upon gradual addition of Ga^{3+} to sensor **1**, UV-vis titration showed that the absorbance at 367 nm decreased while a novel band at 405 nm appeared, until saturation at 14 equiv. of Ga^{3+} (Fig. S9†). In addition, an isosbestic point appeared at 288 nm, indicating the generation of a new stable complex between **1** and Ga^{3+}.

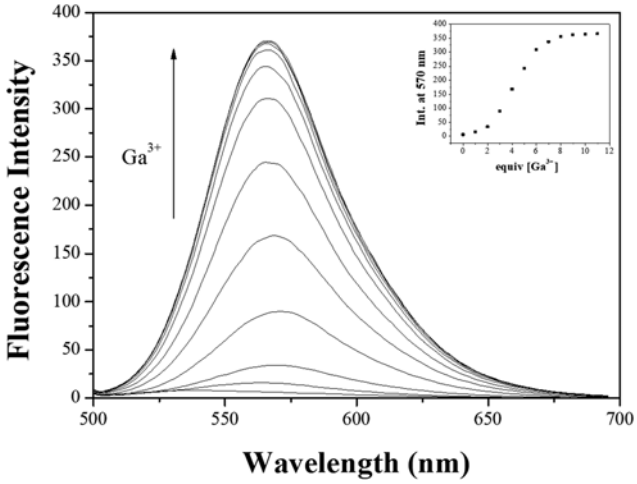

Fig. 5 Fluorescence spectral changes of **1** (20 μM) in the presence of different concentrations of Ga^{3+} ions, with an excitation of 481 nm. Inset: Fluorescence intensity at 570 nm *versus* the number of 10 equiv. of Ga^{3+} added.

To determine the binding stoichiometry of **1** to Ga^{3+}, Job plot analysis was carried out, which indicated formation of a 2 : 1 complex between **1** and Ga^{3+} (Fig. S10†).[63] To better confirm the coordination mode of **1** to Ga^{3+}, ESI-MS analysis of probe **1** in the presence of Ga^{3+} was performed. As shown in Fig. S11,† a peak at m/z = 889.29 could be assigned to [2·**1** + Ga^{3+}-2H^{+}]$^{+}$ (calcd 889.23). On the basis of these observations, a possible coordination mode between **1** and Ga^{3+} is proposed in Scheme 2. The association constant (K) of the Ga^{3+}-2·**1** complex was determined to be 5.0×10^{7} M^{-2} by Li's equation using the fluorescence titration data (Fig. S12†).[64] Importantly,

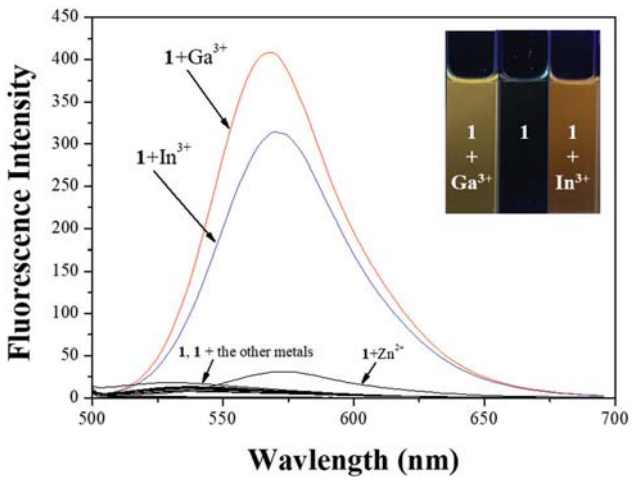

Fig. 4 Fluorescence spectral changes of **1** (20 μM) in the presence of different metal ions (10 equiv. Zn^{2+}, Cd^{2+}, In^{3+}, Cu^{2+}, Fe^{2+}, K^{+}, Na^{+}, Mg^{2+}, Pb^{2+}, Cr^{3+}, Co^{2+}, Ni^{2+}, Fe^{3+}, Ca^{2+}, Mn^{2+}, Al^{3+}, Ga^{3+}, Ag^{+} and Hg^{2+}) with an excitation of 481 nm.

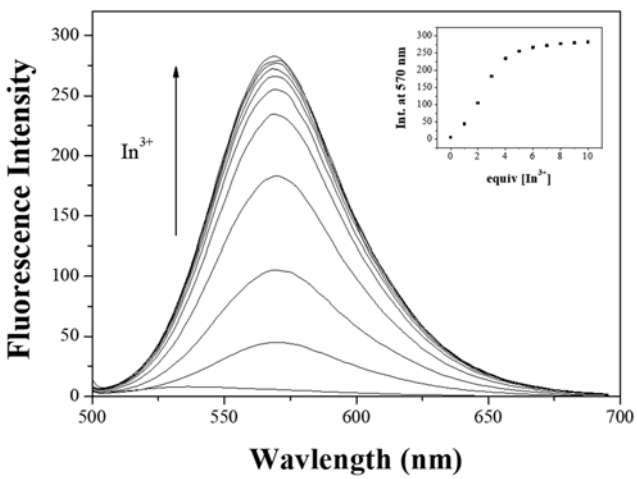

Fig. 6 Fluorescence spectral changes of **1** (20 μM) in the presence of different concentrations of In^{3+} ions, with an excitation of 481 nm. Inset: Fluorescence intensity at 570 nm *versus* the number of 9 equiv. of In^{3+} added.

the association constant is the highest reported to date for a chemosensor for the detection of Ga^{3+}.[23,25–27,47,50,66]

To check the fluorescence selectivity of probe **1** for Ga^{3+} in the presence of competing metal ions, competition experiments were carried out (Fig. S13†). Most of the competing metal ions did not interfere with the detection of Ga^{3+}, which may be attributed to the stability of the complex of **1** with Ga^{3+}. However, Fe^{2+}, Cu^{2+} and Mg^{2+} inhibited the fluorescence emission of the Ga^{3+}-2·**1** species. These results indicated that sensor **1** could selectively bind to Ga^{3+} without any interference from most metal ions.

Next, fluorescence titration was performed to examine the detecting ability of probe **1** towards In^{3+} (Fig. 6). When probe **1** was titrated with In^{3+} ions, the fluorescence emission steadily increased, until saturation at 9 equiv. of In^{3+} ions. To further investigate the interactions between **1** and In^{3+}, UV-vis absorption titration was carried out (Fig. 7). Upon titration of increasing concentrations of In^{3+} (0–3.6 equiv.) against sensor **1** solution, the absorbance at 367 nm decreased, while a novel red-shifted absorption band at 396 nm gradually appeared. When the amount of In^{3+} was beyond 3.2 equiv., the absorbance was saturated, with one isosbestic point at 261 nm, indicating a definite conversion of **1** to an In^{3+} complex.

To determine the binding ratio of probe **1** with In^{3+}, Job plot analysis was conducted (Fig. S14†).[63] The maximum absorbance was found to be at a mole fraction ($[In^{3+}]/([\mathbf{1}] + [In^{3+}])$) of 0.3, indicating a 2 : 1 binding ratio between probe **1** and In^{3+}. This result was consistent with the ESI-MS analysis (Fig. 8). The positive-ion mass suggested the formation of $[2\cdot\mathbf{1} + In^{3+}\text{-}2H^{+}]^{+}$, based on the presence of a peak at m/z = 935.32 (calcd 935.20). The association constant was determined to be 1.0×10^{8} M^{-2} according to Li's equation (Fig. S15†).[64] Importantly, the association constant is the highest reported to date for a chemosensor for detection of In^{3+} (Table S1†). The detection limit for In^{3+} was calculated to be 7.92 μM based on 3σ/slope analysis (Fig. S16†).[65] On the basis of ESI-MS, Job plot analysis, and UV-vis titration, a probable structure for the In^{3+}-2·**1** complex is proposed in Scheme 2.

The preferential selectivity of probe **1** towards In^{3+} was evaluated *via* fluorescence competition experiments over various competing metal ions (Fig. S17†). Most of the coexisting cations showed no or negligible interference with the fluorescence intensity of the In^{3+}-2·**1** complex, except Cu^{2+}, Al^{3+}, Fe^{2+}, Cr^{3+} and Fe^{3+}. Cu^{2+} and Al^{3+} reduced the fluorescence intensity by about half, and Fe^{2+}, Fe^{3+} and Cr^{3+} showed interference of more than 90% because of their intrinsic fluorescence quenching properties.[67,68]

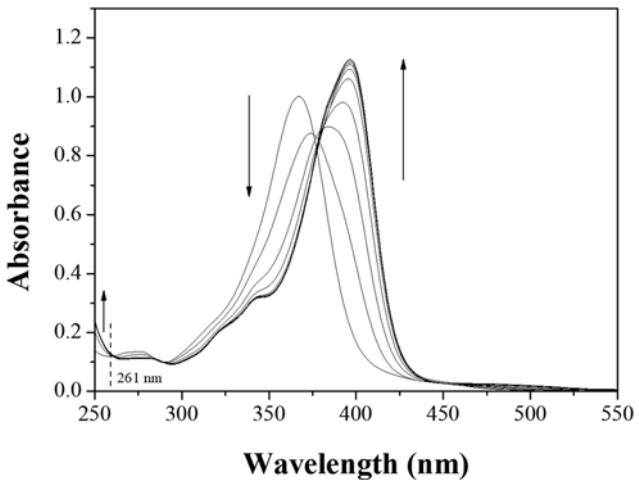

Fig. 7 UV-vis spectral changes of **1** (20 μM) in the presence of different concentrations of In^{3+} ions.

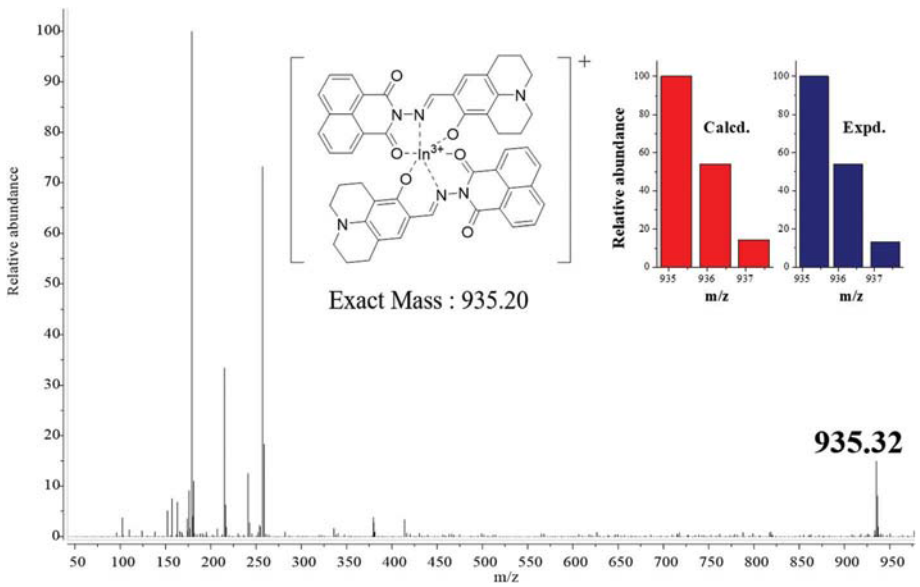

Fig. 8 Positive-ion ESI-MS of sensor **1** (0.1 mM) with $In(NO_3)_3$ (1.0 equiv.).

3.3. Theoretical calculations for Al^{3+}-2·1, Ga^{3+}-2·1 and In^{3+}-2·1 complexes

We carried out DFT and TD-DFT calculations to further investigate sensing mechanisms of Al^{3+}-2·**1**, Ga^{3+}-2·**1** and In^{3+}-2·**1** complexes. All calculations were performed with a 2 : 1 stoichiometric ratio between **1** and metal ions, based on experimental data. For **1**, the energy-optimized structure showed a twisted shape with a dihedral angle of 109.939° (1O, 2C, 3C, 4O) (Fig. 9(a)). For all complexes, the structures indicated that Al^{3+}, Ga^{3+} and In^{3+} were bound to the oxygen atoms of the naphthalic and the julolidine moieties and the nitrogen atoms of the imine moieties of 2·**1** (Fig. 9(b)–(d)). Binding mechanisms of Al^{3+}-2·**1**, Ga^{3+}-2·**1** and In^{3+}-2·**1** complexes were examined using TD-DFT calculations. For **1**, the 4th excited state of MO contribution was analyzed to be the HOMO → LUMO+1 and HOMO−2 → LUMO transitions (342.30 nm, Fig. S18†), which were characterized to the π → π* transition. For Al^{3+}-2·**1**, the 11th excited state of MO contribution was analyzed to be HOMO → LUMO+2 and HOMO → LUMO+3 transitions (393.28 nm, Fig. S19†). For Ga^{3+}-2·**1**, the 12th excited state of MO contribution was analyzed to be HOMO−1 → LUMO+3

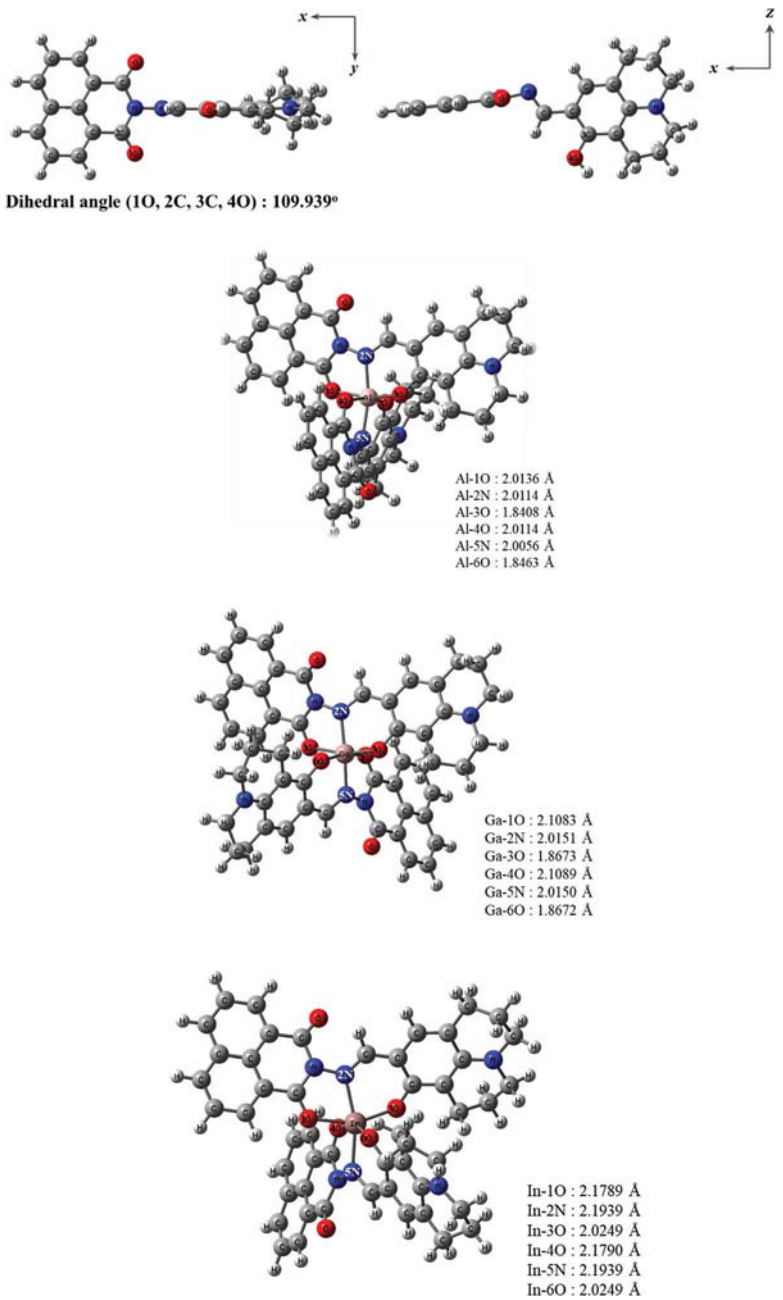

Fig. 9 Energy-minimized structures for (a) **1**, (b) Al^{3+}-2·**1**, (c) Ga^{3+}-2·**1** and (d) In^{3+}-2·**1** complexes.

and HOMO → LUMO+2 transitions (384.10 nm, Fig. S20†). For In^{3+}-2·**1**, the 12th excited state of MO contribution was analyzed to be HOMO → LUMO+3 and HOMO−1 → LUMO+2 transitions (387.68 nm, Fig. S21†). All complexes exhibited intramolecular charge transfer (ICT) from the julolidine moieties to the naphthalic and imine ones (Fig. S22†). These results suggested that the occurrence of ICT transitions upon the chelating between **1** and the metal ions Al^{3+}, Ga^{3+} and In^{3+} led to the increase of fluorescence intensity of **1**. Based on the experimental data (ESI-MS and Job plot analyses) and theoretical calculations, the binding mechanisms of Al^{3+}-2·**1**, Ga^{3+}-2·**1** and In^{3+}-2·**1** complexes are proposed in Scheme 2.

4. Conclusion

We present a novel multifunctional fluorescent probe **1**, which exhibits high selectivity for trivalent ions (Al^{3+}, Ga^{3+} and In^{3+}). The sensor could simultaneously sense and differentiate between Al^{3+}, Ga^{3+} and In^{3+} through turn-on fluorescence at different wavelengths. Binding modes of 2 : 1 for **1** with Al^{3+}, Ga^{3+} and In^{3+} are proposed based on Job plots and ESI-MS. The association constants of Ga^{3+}-2·**1** and In^{3+}-2·**1** complex are the highest reported to date for a chemosensor for these ions. Importantly, this is the first report to our knowledge that a chemosensor can selectively detect and differentiate between Al^{3+}, In^{3+} and Ga^{3+}, while several chemosensors reported to date have difficulty in distinguishing between Al^{3+}, In^{3+} and Ga^{3+} because of the similar behaviors of these ions. Thus, these results provide new insight into the development of novel multifunctional probes for distinguishing between metal ions in the same group.

Conflicts of interest

There are no conflicts to declare.

Acknowledgements

This work was supported by a National Research Foundation of Korea Grant (NRF-2018R1A2B6001686) and the Korea Ministry of Environment (MOE) as "The Chemical Accident Prevention Technology Development Project" (no. 2016001970001).

References

1 T. Kawano, T. Kadono, T. Furuichi, S. Muto and F. Lapeyrie, Aluminum-induced distortion in calcium signaling involving oxidative bursts and channel regulation in tobacco BY-2 cells, *Biochem. Biophys. Res. Commun.*, 2003, **308**, 35–42.

2 S. Paul, A. Manna and S. Goswami, A differentially selective molecular probe for detection of trivalent ions (Al3+, Cr^{3+} and Fe^{3+}) upon single excitation in mixed aqueous medium, *Dalton Trans.*, 2015, **44**, 11805–11810.

3 T. H. Y. Jeong, S. Y. Lee, J. Han, M. H. Lim and C. Kim, Thiophene and diethylaminophenol-based "turn-on" fluorescence chemosensor for detection of Al^{3+} and F^- in a near-perfect aqueous solution, *Tetrahedron*, 2017, **73**, 2690–2697.

4 T. G. Jo, J. J. Lee, E. Nam, K. H. Bok, M. H. Lim and C. Kim, A highly selective fluorescent sensor for the detection of Al^{3+} and CN^- in aqueous solution: biological applications and DFT calculations, *New J. Chem.*, 2016, **40**, 8918–8927.

5 E. Delhaize and P. R. Ryan, Aluminum Toxicity and Tolerance in Plants, *Plant Physiol.*, 1995, **107**, 315–321.

6 D. L. Godbold, E. Fritz and A. Hüttermann, Aluminum toxicity and forest decline, *Proc. Natl. Acad. Sci. U. S. A.*, 1988, **85**, 3888–3892.

7 L. Kang, Z.-Y. Xing, X.-Y. Ma, Y.-T. Liu and Y. Zhang, A highly selective colorimetric and fluorescent turn-on chemosensor for Al^{3+} based on naphthalimide derivative, *Spectrochim. Acta, Part A*, 2016, **167**, 59–65.

8 C. Liang, W. Bu, C. Li, G. Men, M. Deng, Y. Jiangyao, H. Sun, S. Jiang, S.-T. Lee, J. Kim, V. Marcelino, P. Paoletti and B. Valtancoli, A highly selective fluorescent sensor for Al^{3+} and the use of the resulting complex as a secondary sensor for PPi in aqueous media: its applicability in live cell imaging, *Dalton Trans.*, 2015, **44**, 11352–11359.

9 S. Goswami, S. Paul and A. Manna, Selective "naked eye" detection of Al(III) and PPi in aqueous media on a rhodamine–isatin hybrid moiety, *RSC Adv.*, 2013, **3**, 10639–10643.

10 Y. W. Choi, G. J. Park, Y. J. Na, H. Y. Jo, S. A. Lee, G. R. You and C. Kim, A single schiff base molecule for recognizing multiple metal ions: A fluorescence sensor for Zn(II) and Al(III) and colorimetric sensor for Fe(II) and Fe(III), *Sens. Actuators, B*, 2014, **194**, 343–352.

11 F. Wang, H. Duan, D. Xing and G. Yang, Novel Turn-on Fluorescence Probes for Al^{3+} Based on Conjugated Pyrazole Schiff Base, *J. Fluoresc.*, 2017, **27**, 1721–1727.

12 J. Kawakami, A. Tsuiki, S. Ito and H. Kitahara, Naphthalene Ring-Fused 2-Aminotryptanthrin as a Fluorescent Chemosensor for Al^{3+}, *Trans. Mater. Res. Soc. Jpn.*, 2016, **41**, 131–133.

13 M. Li, X. Zhang, Y.-h. Fan and C. Bi, A novel fluorescent probe based on rhodamine hydrazone derivatives bearing a thiophene group for Al^{3+}, *Luminescence*, 2016, **31**, 851–855.

14 Q. Wang, L. Yang, H. Wang, J. Song, H. Ding, X.-H. Tang and H. Yao, A highly selective and sensitive turn-on fluorescent probe for the detection of Al^{3+} and its bioimaging, *Luminescence*, 2017, **32**, 779–785.

15 D. Maity and T. Govindaraju, Conformationally Constrained (Coumarin−Triazolyl−Bipyridyl) Click Fluoroionophore as a Selective Al^{3+} Sensor, *Inorg. Chem.*, 2010, **49**, 7229–7231.

16 I. H. Hwang, Y. W. Choi, K. B. Kim, G. J. Park, J. J. Lee, L. Nguyen, I. Noh and C. Kim, A highly selective and sensitive fluorescent turn-on Al^{3+} chemosensor in aqueous media and living cells: experimental and theoretical studies, *New J. Chem.*, 2016, **40**, 171–178.

17 P. Torawane, K. Tayade, S. Bothra, S. K. Sahoo, N. Singh, A. Borse and A. Kuwar, A highly selective and sensitive fluorescent "turn-on" chemosensor for Al^{3+} based on CN isomerisation mechanism with nanomolar detection, *Sens. Actuators, B*, 2016, **222**, 562–566.

18 F. Yu, L. J. Hou, L. Y. Qin, J. B. Chao, Y. Wang and W. J. Jin, A new colorimetric and turn-on fluorescent chemosensor for Al^{3+} in aqueous medium and its application in live-cell imaging, *J. Photochem. Photobiol., A*, 2016, **315**, 8–13.

19 C. Li, J. Qin, B. Wang, X. Bai and Z. Yang, Fluorescence chemosensor properties of two coumarin-based compounds for environmentally and biologically important Al^{3+} ion, *J. Photochem. Photobiol., A*, 2017, **332**, 141–149.

20 A. Tanaka, Toxicity of indium arsenide, gallium arsenide, and aluminium gallium arsenide, *Toxicol. Appl. Pharmacol.*, 2004, **198**, 405–411.

21 C. R. Chitambar, Medical Applications and Toxicities of Gallium Compounds, *Int. J. Environ. Res. Public Health*, 2010, **7**, 2337–2361.

22 D. P. Kelsen, N. Alcock, S. Yeh, J. Brown and C. Young, Pharmacokinetics of gallium nitrate in man, *Cancer*, 1980, **46**, 2009–2013.

23 D. Kara, A. Fisher, M. Foulkes and S. Hill, Determination of gallium at trace levels using a spectrofluorimetric method in synthetic U–Ga and Ga–As solutions, *Spectrochim. Acta, Part A*, 2010, **75**, 361–365.

24 H. Tavallali, P. Vahdati and E. Shaabanpur, Developing a new method of 4-(2-pyridylazo)-resorcinol immobilization on triacetylcellulose membrane for selective determination of Ga^{3+} in water samples, *Sens. Actuators, B*, 2011, **159**, 154–158.

25 L. Yan, Y. Zhou, W. Du, Z. Kong and Z. Qi, A new turn on coumarin-based fluorescence probe for Ga^{3+} detection in aqueous solution, *Spectrochim. Acta, Part A*, 2016, **155**, 116–124.

26 Z. Zeng, R. Ma, C. Liu, Y. Xu, H. Li, F. Liu and S. Sun, A crab-like fluorescent probe for Ga(III) detection in body fluids and biological tissues, *Sens. Actuators, B*, 2017, **250**, 267–273.

27 C. Lim, M. An, H. Seo, J. H. Huh, A. Pandith, A. Helal and H.-S. Kim, Fluorescent probe for sequential recognition of Ga^{3+} and pyrophosphate anions, *Sens. Actuators, B*, 2017, **241**, 789–799.

28 A. J. Downs, *Chemistry of aluminium, gallium, indium, and thallium*, Blackie Academic & Professional, 1993.

29 D. Y. Han, J. M. Kim, J. Kim, H. S. Jung, Y. H. Lee, J. F. Zhang and J. S. Kim, ESIPT-based anthraquinonylcalix[4]crown chemosensor for In^{3+}, *Tetrahedron Lett.*, 2010, **51**, 1947–1951.

30 Y.-C. Wu, H.-J. Li and H.-Z. Yang, A sensitive and highly selective fluorescent sensor for In^{3+}, *Org. Biomol. Chem.*, 2010, **8**, 3394–3397.

31 Y.-M. Kho and E. J. Shin, Spiropyran-Isoquinoline Dyad as a Dual Chemosensor for Co(II) and In(III) Detection, *Molecules*, 2017, **22**, 1569–1582.

32 H. Kim, K. B. Kim, E. J. Song, I. H. Hwang, J. W. Noh, P. G. Kim, K. D. Jeong and C. Kim, Turn-on selective fluorescent probe for trivalent cations, *Inorg. Chem. Commun.*, 2013, **36**, 72–76.

33 D. Maity and T. Govindaraju, A differentially selective sensor with fluorescence turn-on response to $Zn2^{+}$ and dual-mode ratiometric response to Al^{3+} in aqueous media, *Chem. Commun.*, 2012, **48**, 1039–1041.

34 G. J. Park, I. H. Hwang, E. J. Song, H. Kim and C. Kim, A colorimetric and fluorescent sensor for sequential detection of copper ion and cyanide, *Tetrahedron*, 2014, **70**, 2822–2828.

35 G. J. Park, G. R. You, Y. W. Choi and C. Kim, A naked-eye chemosensor for simultaneous detection of iron and copper ions and its copper complex for colorimetric/fluorescent sensing of cyanide, *Sens. Actuators, B*, 2016, **229**, 257–271.

36 H. Liu, B. Zhang, C. Tan, F. Liu, J. Cao, Y. Tan and Y. Jiang, Simultaneous bioimaging recognition of Al^{3+} and Cu^{2+} in living-cell, and further detection of F^{-} and S^{2-} by a simple fluorogenic benzimidazole-based chemosensor, *Talanta*, 2016, **161**, 309–319.

37 Z. Liao, Y. Liu, S.-F. Han, D. Wang, J.-Q. Zheng, X.-J. Zheng and L.-P. Jin, A novel acylhydrazone-based derivative as dual-mode chemosensor for Al^{3+}, $Zn2^{+}$ and Fe^{3+} and its applications in cell imaging, *Sens. Actuators, B*, 2017, **244**, 914–921.

38 Y. Yang, C.-Y. Gao, N. Zhang and D. Dong, Tetraphenylethene functionalized rhodamine chemosensor for Fe^{3+} and Cu^{2+} ions in aqueous media, *Sens. Actuators, B*, 2016, **222**, 741–746.

39 A. Roy, S. Dey and P. Roy, A ratiometric chemosensor for Al^{3+} based on naphthalene-quinoline conjugate with the resultant complex as secondary sensor for F^{-}: Interpretation of molecular logic gates, *Sens. Actuators, B*, 2016, **237**, 628–642.

40 W. Zhu, L. Yang, M. Fang, Z. Wu, Q. Zhang, F. Yin, Q. Huang and C. Li, New carbazole-based Schiff base: Colorimetric chemosensor for Fe^{3+} and fluorescent turn-on chemosensor for Fe^{3+} and Cr^{3+}, *J. Lumin.*, 2015, **158**, 38–43.

41 S. Goswami, K. Aich, S. Das, A. K. Das, D. Sarkar, S. Panja, T. K. Mondal and S. Mukhopadhyay, A red fluorescence "off–on" molecular switch for selective detection of Al^{3+}, Fe^{3+} and Cr^{3+}: experimental and theoretical studies along with living cell imaging, *Chem. Commun.*, 2013, **49**, 10739–10741.

42 T. G. Jo, J. M. Jung, J. Han, M. H. Lim and C. Kim, A single fluorescent chemosensor for multiple targets of Cu^{2+}, $Fe2^{+}/^{3+}$ and Al^{3+} in living cells and a near-perfect aqueous solution, *RSC Adv.*, 2017, **7**, 28723–28732.

43 S. Goswami, A. Manna, S. Paul, A. K. Maity, P. Saha, C. K. Quah and H.-K. Fun, FRET based "red-switch" for Al^{3+} over ESIPT based "green-switch" for Zn^{2+}: dual channel detection with live-cell imaging on a dyad platform, *RSC Adv.*, 2014, **4**, 34572–34576.

44 H.-S. Kim, S. Angupillai and Y.-A. Son, A dual chemosensor for both Cu^{2+} and Al^{3+}: A potential Cu^{2+} and Al^{3+} switched YES logic function with an INHIBIT logic gate and a novel

solid sensor for detection and extraction of Al^{3+} ions from aqueous solution, *Sens. Actuators, B*, 2016, **222**, 447–458.
45 R. Purkait, C. Patra, A. Das Mahapatra, D. Chattopadhyay and C. Sinha, A visible light excitable chromone appended hydrazide chemosensor for sequential sensing of Al^{3+} and F^- in aqueous medium and in Vero cells, *Sens. Actuators, B*, 2018, **257**, 545–552.
46 M. Lo Presti, S. El Sayed, R. Martínez-Máñez, A. M. Costero, S. Gil, M. Parra and F. Sancenón, Selective chromo-fluorogenic detection of trivalent cations in aqueous environments using a dehydration reaction, *New J. Chem.*, 2016, **40**, 9042–9045.
47 S. Y. Lee, K. H. Bok, T. G. Jo, S. Y. Kim and C. Kim, A simple Schiff-base fluorescence probe for the simultaneous detection of Ga^{3+} and Zn^{2+}, *Inorg. Chim. Acta*, 2017, **461**, 127–135.
48 Y.-W. Wang, S.-B. Liu, W.-J. Ling and Y. Peng, A fluorescent probe for relay recognition of homocysteine and Group IIIA ions including Ga(III), *Chem. Commun.*, 2016, **52**, 827–830.
49 B.-Y. Kim, H.-S. Kim and A. Helal, A fluorescent chemosensor for sequential recognition of gallium and hydrogen sulfate ions based on a new phenylthiazole derivative, *Sens. Actuators, B*, 2015, **206**, 430–434.
50 B. Tang, Z.-Z. Chen, N. Zhang, J. Zhang and Y. Wang, Synthesis and characterization of a novel cross-linking complex of β-cyclodextrin-o-vanillin furfuralhydrazone and highly selective spectrofluorimetric determination of trace gallium, *Talanta*, 2006, **68**, 575–580.
51 K. Xiong, F. Huo, C. Yin, J. Chao, Y. Zhang and M. Xu, A highly selective fluorescent bioimaging probe for hypochlorite based on 1,8-naphthalimide derivative, *Sens. Actuators, B*, 2015, **221**, 1508–1514.
52 M. J. Frisch, G. W. Trucks, H. B. Schlegel, G. E. Scuseria, M. A. Robb, J. R. Cheeseman, G. Scalmani, V. Barone, B. Mennucci, G. A. Petersson, H. Nakatsuji, M. Caricato, X. Li, H. P. Hratchian, A. F. Izmaylov, J. Bloino, G. Zheng, J. L. Sonnenberg, M. Hada, M. Ehara, K. Toyota, R. Fukuda, J. Hasegawa, M. Ishida, T. Nakajima, Y. Honda, O. Kitao, H. Nakai, T. Vreven, J. A. Montgomery Jr., J. E. Peralta, F. Ogliaro, M. Bearpark, J. J. Heyd, E. Brothers, K. N. Kudin, V. N. Staroverov, R. Kobayashi, J. Normand, K. Raghavachari, A. Rendell, J. C. Burant, S. S. Iyengar, J. Tomasi, M. Cossi, N. Rega, J. M. Millam, M. Klene, J. E. Knox, J. B. Cross, V. Bakken, C. Adamo, J. Jaramillo, R. Gomperts, R. E. Stratmann, O. Yazyev, A. J. Austin, R. Cammi, C. Pomelli, J. W. Ochterski, R. L. Martin, K. Morokuma, V. G. Zakrzewski, G. A. Voth, P. Salvador, J. J. Dannenberg, S. Dapprich, A. D. Daniels, Ö. Farkas, J. B. Foresman, J. V. Ortiz, J. Cioslowski and D. J. Fox, *Gaussian 09*, Gaussian, Inc., Wallingford CT, 2009.
53 A. D. Becke, Density-functional thermochemistry. III. The role of exact exchange, *J. Chem. Phys.*, 1993, **98**, 5648–5652.
54 C. Lee, W. Yang and R. G. Parr, Development of the Colle-Salvetti correlation-energy formula into a functional of the electron density, *Phys. Rev. B: Condens. Matter Mater. Phys.*, 1988, **37**, 785–789.
55 P. C. Hariharan and J. A. Pople, The influence of polarization functions on molecular orbital hydrogenation energies, *Theor. Chim. Acta*, 1973, **28**, 213–222.
56 M. M. Francl, W. J. Pietro and W. J. Hehre, Self-consistent molecular orbital methods. XXIII. A polarization-type basis set for second-row elements, *J. Chem. Phys.*, 1982, **77**, 3654–3665.
57 P. J. Hay and W. R. Wadt, Ab initio effective core potentials for molecular calculations. Potentials for the transition metal atoms Sc to Hg, *J. Chem. Phys.*, 1985, **82**, 270–283.
58 W. R. Wadt and P. J. Hay, Ab initio effective core potentials for molecular calculations. Potentials for main group elements Na to Bi, *J. Chem. Phys.*, 1985, **82**, 284–298.
59 P. J. Hay and W. R. Wadt, Ab initio effective core potentials for molecular calculations. Potentials for K to Au including the outermost core orbitals, *J. Chem. Phys.*, 1985, **82**, 299–310.
60 V. Barone and M. Cossi, Quantum Calculation of Molecular Energies and Energy Gradients in Solution by a Conductor Solvent Model, *J. Phys. Chem. A*, 1998, **102**, 1995–2001.
61 M. Cossi and V. Barone, Time-dependent density functional theory for molecules in liquid solutions, *J. Chem. Phys.*, 2001, **115**, 4708–4717.
62 N. M. O'boyle, A. L. Tenderholt and K. M. Langner, cclib: A library for package-independent computational chemistry algorithms, *J. Comput. Chem.*, 2008, **29**, 839–845.
63 P. Job, Formation and stability of inorganic complexes in solution, *Ann. Chim.*, 1928, **9**, 113–203.
64 R. Yang, K. Li, K. Wang, F. Zhao, N. Li and F. Liu, Porphyrin Assembly on β-Cyclodextrin for Selective Sensing and Detection of a Zinc Ion Based on the Dual Emission Fluorescence Ratio, *Anal. Chem.*, 2003, **75**, 612–621.
65 Y.-K. Tsui, S. Devaraj and Y.-P. Yen, Azo dyes featuring with nitrobenzoxadiazole (NBD) unit: A new selective chromogenic and fluorogenic sensor for cyanide ion, *Sens. Actuators, B*, 2012, **161**, 510–519.
66 J. Kimura, H. Yamada, H. Ogura, T. Yajima and T. Fukushima, Development of a fluorescent chelating ligand for gallium ion having a quinazoline structure with two Schiff base moieties, *Anal. Chim. Acta*, 2009, **635**, 207–213.
67 Z. Liu, Z. Yang, T. Li, B. Wang, Y. Li, D. Qin, M. Wang and M. Yan, An effective Cu(II) quenching fluorescence sensor in aqueous solution and 1D chain coordination polymer framework, *Dalton Trans.*, 2011, **40**, 9370–9373.
68 Q. Mei, C. Jiang, G. Guan, K. Zhang, B. Liu, R. Liu and Z. Zhang, Fluorescent graphene oxide logic gates for discrimination of iron (3+) and iron (2+) in living cells by imaging, *Chem. Commun.*, 2012, **48**, 7468–7470.